Research Article

Sinan A. Al-Haddad, Mohammed Y. Fattah, Thamir K. Al-Azawi and Luttfi A. Al-Haddad*

Three-dimensional analysis of steel beam-column bolted connections

https://doi.org/10.1515/eng-2022-0579 received November 01, 2023; accepted January 09, 2024

Abstract: The design of steel beam-column end-plate bolted connections is becoming increasingly popular owing to its simplicity of production. This requires knowledge of the full nonlinear resisting moment-rotation (M-Φ) behavior of the joint. To investigate the impact of various geometrical factors on the overall behavior of the connection, this work provides a three-dimensional finite element model (FEM) utilizing ABAQUS software. The suggested model accounts for the pretension force on the bolts, material and geometrical deviations from linearity, and the proximity of surfaces that are adjacent. The numerical model's ability to simulate and process both the total and specific behavior of varieties of end-plate steel riveted connections is confirmed by calibrating the finite element findings with experimentally disclosed outcomes, which are reviewed in this study. The ultimate behavior was then investigated through a parametric study using the verified FEM with variations in the bolt pretension load, yield strength of the sections, and yield stress of the bolt considering the $M-\Phi$ curve. The results of the parametric study showed that as the bolt pretension load and yield stress of the column, beam, and plate materials increased, so did the connection's moment ability. The yield tension of the bolts, however, had only a minor effect on the connection's moment capacity.

Keywords: finite element analysis, end-plate steel connections, bolted connections, bolts pretension load, moment-rotation $(M-\Phi)$

e-mail: Luttfi.A.AlHaddad@uotechnology.edu.iq

Sinan A. Al-Haddad: Civil Engineering Department, University of Technology-Iraq, Baghdad, Iraq,

e-mail: Sinan.A.AlHaddad@uotechnology.edu.iq

Mohammed Y. Fattah: Civil Engineering Department, University of Technology-Iraq, Baghdad, Iraq, e-mail: myf_1968@yahoo.com

Thamir K. Al-Azawi: Building and Construction Technology Enginnering, Al-Esraa University, Baghdad, Iraq, e-mail: dr.thamer@esraa.edu.iq

1 Introduction

Several research studies have been published related to the finite element analysis (FEA) of steel connections to simulate and investigate the behavior of such connections. The rationale behind this is that it is believed to have advantages over fully experimental testing and maintaining good connection actions in terms of time and cost savings. Some of these numerical models were given in previous studies [1–5]. All the aforementioned researchers modeled and simulated the behavior of steel end-plate connections via FEA to study and analyze the behavior of these connections using various FEA software packages such as ABAQUS and ANSYS. In addition, the numerical results were compared and validated using experimental results.

Numerous studies have adopted analytical and experimental research on end-plate steel connections to develop a reliable approach for predicting the rotational attitude of the connection under monotonic and cyclic stresses. To calculate the initial rotational stiffness of semi-rigid joints, Dabaon [6] proposed a fundamental method based on Euro Code 3 [7]. In a review study, Dabaon [8] defined the grouping of beam-to-column junctions. The researcher conducted the composite joint study after the addition of everything. A novel exponential model was created by Mohamadi-Shoore and Mofid [9] to estimate the regular M-curves of bolted end-plate connections.

Shi et al. [10] introduced a recent theoretical approach to evaluate the moment–rotation (M– Φ) relation for reinforced and lengthened beam-column end-plate connections. The end-plate connection is split into many components, which include the end-plate, panel area, bolt, or column flange, based on a particular understanding of the rotation of the end-plate connection. The analysis encompasses the whole loading–deformation operation of each segment, hence allowing for the acquisition of the loading–deformation procedure for every connection by the superimposition of the behavior of every segment. Five joint tests were conducted to verify the proposed analytical approach. It was concluded that this analytical approach can precisely determine the M– Φ curve, initial rotational stiffness, and

^{*} Corresponding author: Luttfi A. Al-Haddad, Training and Workshops Center, University of Technology-Iraq, Baghdad, Iraq,

rotational behavior of end-plate connections in comparison with the test data. Additionally, it has the ability to examine any benefit to the rotational deformation of the joint, including twisting deformation of the end-plate and column flange, bolt extension, and shear deformation of the panel zone.

The experimental findings of eight segments of steelbolted connections beam-to-beam and beam-to-column with flush or extended end-plates were given by Abidelah et al. [11]. Fifty percent of the connections have end-plates that have been reinforced with stiffeners in the extended sections. The study used a column with low resistance to investigate the interplay of failure mechanisms in both the compression and tension zones. The analysis focused on evaluating the global M-Φ curves and the concurrent development of tension forces in the bolts. The primary metrics that were observed were failure mechanisms, stiffness, resistance development, and rotation capacity. A comprehensive analysis was performed to compare the experimental and analytical findings obtained from the component method of Eurocode 3. The objective was to assess the precision of the analytical methodology, particularly in relation to the connections involving stiffeners in the extended section of the end-plates.

Using the fixable program ABAQUS, Ismail et al. [12] presented a three-dimensional FEM to examine the impact of different geometrical factors on the attitude and behavior of the connection. The recommended model considers material and geometrical nonlinearities, pretension force in the bolts, contact between adjacent surfaces, and initial flaws. The experimental calibration and analysis of the finite element results demonstrated that the numerical system was capable of simulating the general and specific attitudes of several types of bolted end-plate steel connections. The parametric analysis also analyzed the final behavior and attitude with adjustments to the bolt diameter, end-plate thickness, column stiffener length, and rib stiffener angle. The findings were examined and put to the test with regard to the mechanisms of failure, the evolution of the resistance, the starting stiffness, and the capacity for rotation.

The results of four full-scale beam-to-column deconstructable composite joint connectors with high-strength steel S690 flush end-plates (FEPs) were presented and discussed by Ataei et al. [13]. They investigated the structural behavior and attitude of the new model in conjunction with the application of post-inducted friction-grip bolted shear connectors for progressing deconstructable composite floors. The test results showed that the composite beam-to-column joints can bring forth the required ductility and strength in accordance with Eurocode 3 and Eurocode 4 specifications. Additionally, the model can be easily

shared as a proof of theory at the conclusion of the framework's service life.

In order to investigate the impact of minor-axis endplate joints on the behavior of major-axis end-plate joints, as well as the interaction between two minor-axis endplate joints, Costa et al. [14] conducted a study on the joint behavior of five different steel beam-to-column end-plate joint configurations. Due to the presence of diverse threedimensional stress conditions inside the unstiffened web of the column, the sub-frames, including one to three beams, were occupied, therefore engaging in mechanical interactions with two or three main and minor axis joints. The assessment of the interactions was conducted by analyzing the M- Φ connections of the joints, connections, and column structure. The research revealed that the impact of minoraxis joints on the stiffness of major-axis joints in the column web under investigation was low. Additionally, the presence of two minor-axis joints resulted in a mutually reinforcing relationship, leading to increased strength and stiffness.

The study performed by Elflah et al. [15] included the implementation of comprehensive experiments on beamto-column joints made of stainless steel. These junctions were then exposed to static monotonic loads. The assessed joint configurations included an attachment with one flush and one extended end-plate; two connections with top and seated cleats; and two connections with top, seated, and web cleats for single-sided beam-to-column couplings. Stainless steel Grade EN 1.4301 was used for all the connected and attached parts, including bolts, angle cleats, and end-plates. The entire M-Φ characteristics for every test were documented, and the experimentally determined stiffness and moment resistance for every joint were compared to the codified provisions of EN1993-1-8. The connections showed exceptional ductility and could withstand loads that were much higher than those predicted by the design requirements for joints made of carbon steel.

Gao et al. [16] studied the structural behavior of beamto-column joints with double-extended end-plate connections both experimentally and numerically. Two stainless steel grades and a joint made of carbon steel grade Q345B were considered. The M-Φ curves were recorded, demonstrating the excellent ductility of the stainless steel joints. The ABAQUS software package was used to create advanced finite element models (FEMs, which were then tested against the test results. The initial rotational stiffness, plastic moment resistance, and rotation capability of the tested joints are used to determine the accuracy of the design code predictions. The current design requirements result in excessively conservative strength predictions for stainless steel joints, according to the findings, as they do not account for the substantial strain hardening and ductility of the material.

Saha et al. [17] performed a numerical analysis of a semi-rigid joint made of stainless steel subjected to monotonic loading. The study involved a top seat with a doubleweb angle beam-column connection. The constructed FEM was initially validated with experimental data using the ABAQUS/CAE FEA program. Subsequently, 13 models were developed to examine the effects of various geometric parameters on the $M-\Phi$ properties of the joint. In this study, the effects of the bolt number, bolt pretension loads, top and seat angle thicknesses, and web angle thickness were investigated. The ultimate moment capacity and initial stiffness were observed to improve when the top-seat angle and web angle thickness increased. However, the rotation slowed at the very end. The moment capacity was enhanced by adding more bolts to the junction between the beam flanges and the topseat angles. However, the bolt pretension load had little to no effect on the $M-\Phi$ behavior of the joint. Future studies of a similar type can make use of the approach used in this study.

A combined experimental and numerical investigation of stainless-steel end-plate connectors was presented by Song et al. [18], with a focus on their final behavior and rotational capacity. Six connection specimens composed of austenitic and lean duplex stainless steels were examined during the experimental phase under monotonic loading. The tests were specifically designed to examine how the connections behave when subjected to substantial deformations on the verge of failure. It was found that the fractures of the stainless-steel bolts and end-plates were closely related to the rotation capacity. A sophisticated FEM suitable for fracture simulation was created during the numerical phase. Material tests for stainless-steel bolts and plates were used to calibrate the constitutive and fracture models that were implemented. The created FEM exhibited a good level of accuracy in forecasting the behavior of the tested connections on the verge of failure. Finally, in order to assess the moment resistance and rotational capacity of the stainless-steel end-plate connectors, physical testing and computational analyses were performed.

The aim of this research is to conduct some recent FEA using the ABAQUS software to validate the accuracy and reliability of the FEA by correlating the M-Φ curves from FEA and experimental results.

2 Application

2.1 Analysis model

A published experimental work for a model of end-plate bolted connections between beam and column has been selected [19]. For this model, a 3D FEA has been carried out using ABAQUUS software. A connection is to be made between the FEM and the experimental results leading to a conclusion about the accuracy and reliability of the FEM.

2.2 Test arrangement

Ostrander [19] performed large-scale testing of beam-tocolumn FEP connections linked to a column flange to better understand the behavior of the connection. Four of the first group of specimens were simulated (similar column and beam sections and without column stiffeners). The steel sections of the columns, beams, and plates are listed in Table 1.

Figure 1 presents an assembled test specimen, which is obtained from Chen [20] Handbook. The dimensions shown were common to all the specimens tested in this program.

Furthermore, the material properties of the columns, beams, plates, and bolts used in this study are listed in Tables 2 and 3.

2.3 Experimental test results

The experimental test results for each of the tested specimens are presented in Figure 2 by plotting the $M-\Phi$ curve. The connection rotation was determined using the difference between the connection rotation and the rotation of the beam.

The $M-\Phi$ curves have revealed that the studied relationships started out linear and then turned out to be non-

Table 1: Test specimens detailing [20]

Test specimen		1	3	4	9
Column		W8 × 28	W8 × 28	W8 × 28	W8 × 28
Beam		W10 × 21	W10 × 21	W10 × 21	W10 × 21
Plate thickness (inch	1)	1/2	3/8	1/4	3/4
Major	ct	0.500	0.500	0.500	0.500
parameters (inch)	cc	0.500	0.500	0.500	0.500
	tp	0.500	0.375	0.250	0.750
	pt	2.500	2.500	2.500	2.500
	gt	3.500	3.500	3.500	3.500
	li	5.000	5.000	5.000	5.000
	gc	3.500	3.500	3.500	3.500
	рс	2.500	2.500	2.500	2.500
Connection type		FEP conne	ctions		
Mode		All bolted	without col	umn stiffen	er

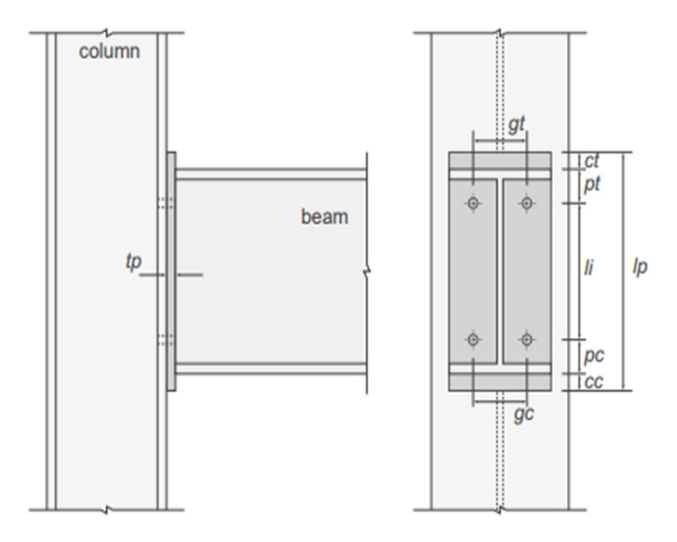


Figure 1: Assembled specimen for J. R. Ostrander experiment model [20].

Table 2: Material properties of columns, beams, and plates [20]

Yield strength, $f_{\rm y}$ (ksi)	Ultimate strength, $f_{ m u}$ (ksi)	Modulus of elasticity, $\it E$ (ksi)
45.4	70.3	30,000

linear. The connections formed a stiff initial response, followed by significantly reduced stiffness in the second applied phase of choice. The inelastic deformation of the attachment components initiated the second step, as per the presented figures.

3 FEM

FEM is majorly considered an asset in computational mechanics in which it provides unmatched applicability and high accuracy in solving diverse challenges and problems in regards to engineering applications [21–29]. FEM plays its rule as an indispensable procedure that captures complicated interactions between assemblies, boundary conditions, and nonlinearities of the components in the context of analyzing the $M-\Phi$ behavior of end-plate bolted steel connections. Traditional analytical methods frequently rely

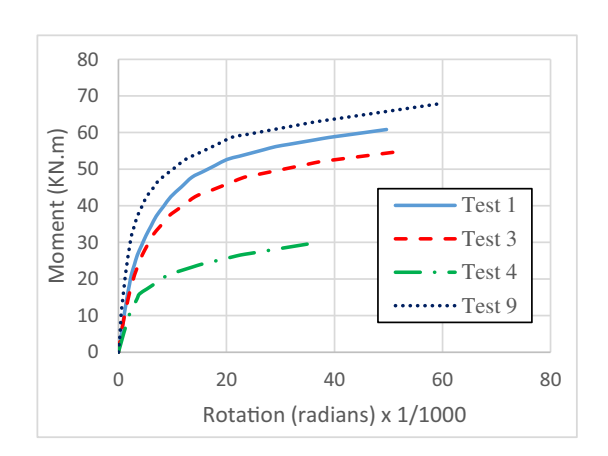


Figure 2: M-Φ for adopted test specimens (Ostrander, [19]).

on simplifications that may not adequately represent real-world conditions, hence introducing potential errors or uncertainties. In contrast to that, FEM permits a more detailed and nuanced analysis that resulted in drawings that closely resemble actual behavior. Consequently, employing FEMs in the analysis of these steel connections would not only improve the reliability of the results, but also substantially contribute to the optimization and safety of structural system design.

ABAQUS software was used for FEM and analysis of the experimental methodology. The accuracy and reliability of the FEM depend on the construction of a suitable mesh arrangement. Mesh discretization must strike a balance between the need for a fine mesh for an accurate stress distribution and the need for a fair analysis period. Using a fine mesh in high-stress areas and a coarser mesh in the rest of the region was the preferred choice. Figure 3 shows a model of the proposed experimental specimens.

The columns, beams, plates, and bolts were modeled using 3D deformable solid shapes. The materials of the model were simulated using nonlinear material properties, and the categories and forms of the generated sections were solid and homogeneous, respectively.

Frictional and welded contacts are considered as interactions. Frictional contact is characterized by establishing interaction: surface-to-surface contact (general) for bolts-to-holes and plate-to-column contact, whereas welded contact is defined by the constraint tie for plate-to-beam welding.

Table 3: Material properties of bolts [20]

Fasteners	Yield strength, $f_{ m y}$ (ksi)	Ultimate strength, $f_{ m u}$ (ksi)	Modulus of elasticity, E (ksi)
A325 (3/4 inch dia.); Standard holes – 13/16 inch	92	120	30,000

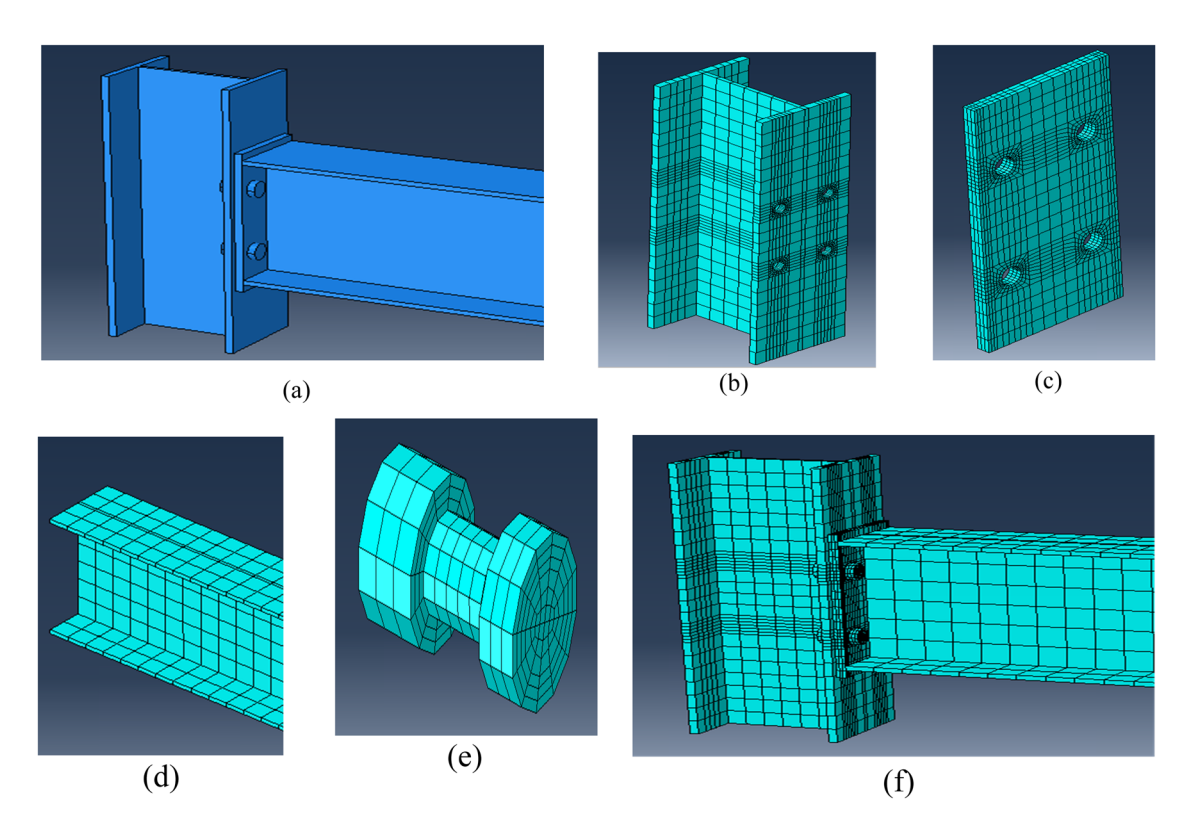


Figure 3: FEM of test specimen: (a) assembled model, (b) meshing of column, (c) meshing of plate, (d) meshing of beam, (e) meshing of bolt, and (f) meshed model.

An 8-node linear brick was adopted for meshing, and the geometric order was linear. Table 4 lists the number of elements.

Nonlinear effects (Nlgeom) were turned on in the phase module to account for the nonlinear effects of massive displacements. The following equation was used to measure the bolt pretension load:

$$T_{\rm b}$$
 = 0.7 × Minimum tensile strength × Area of bolt. (1)

The minimum tensile strength of the bolts was 92,000 psi, and the diameter of the bolt was 3/4 inch.

$$T_{\rm b} = 0.7 \times 92,000 \times \frac{\pi (3/4)^2}{4} = 28,4511b \approx 30,0001b.$$

Table 4: Meshing detailing of the model

Part	Number of elements	
Plate	2,436	
Beam	656	
Column	1,194	
Bolt	600	

3.1 FEA results

Figure 4 shows the results of the FEA of the proposed experimental model.

Two sets of findings were discussed in this report. The data were divided into two categories: experimental test results and results from the FEA. The main purpose of the comparison was to ensure that the FEMs were reliable and trustworthy. As previously stated, FEMs were used to predict the deformation of the relationship. A more precise and figure-based validation is required to ensure the accuracy of FEMs. Figures 5 and 6 demonstrate how the FEM deformation and yield lines (stress concentration) are compared to the experimentally tested deformation.

3.2 Moment resistance

Figures 7-10 show the M-Φ curves of the ABAQUS FEM results. The findings of the M $-\Phi$ curve FEA were compared with the results of experimental experiments. The $M-\Phi$ curves produced by the FEA and experimental M-curves were quite similar.

6 — Sinan A. Al-Haddad et al. DE GRUYTER

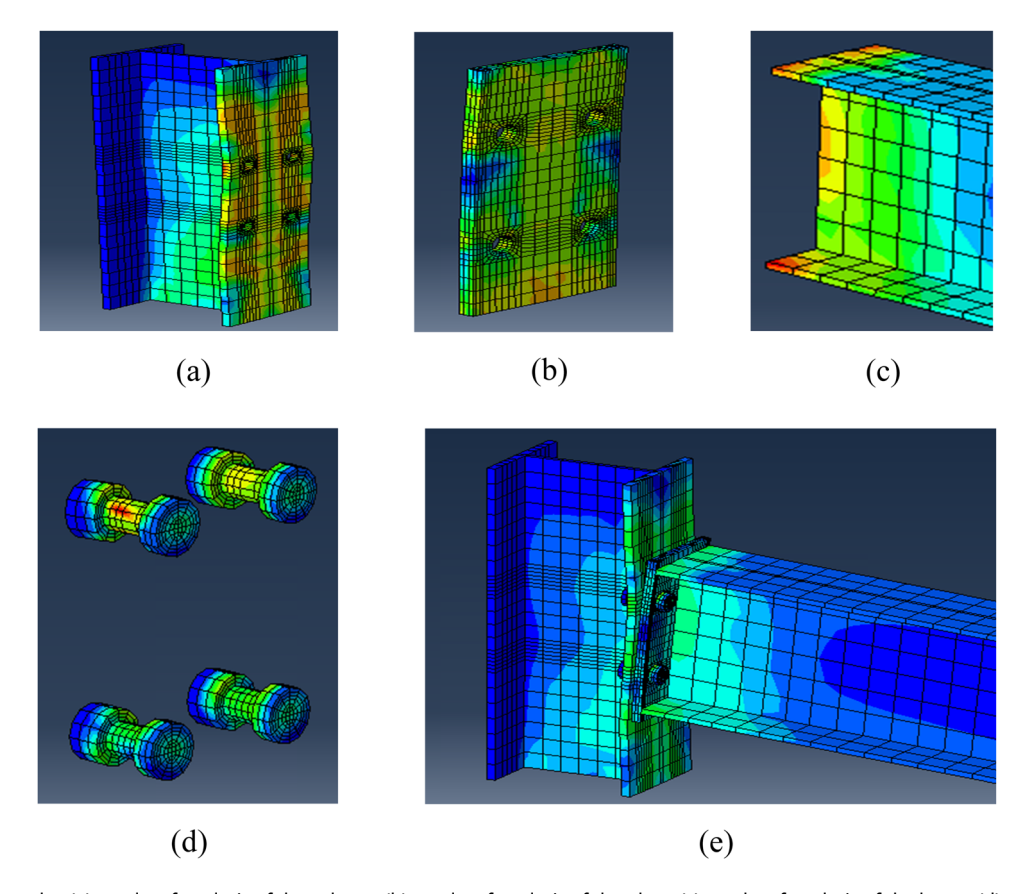


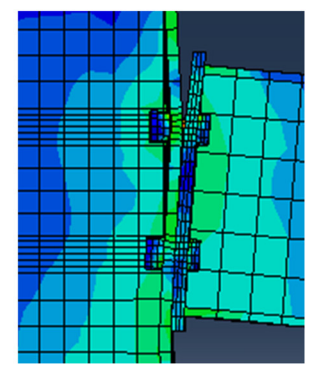
Figure 4: FEM results: (a) results of analysis of the column, (b) results of analysis of the plate, (c) results of analysis of the beam, (d) results of analysis of the bolts, and (e) results of analysis of the assembled model.

The FEA findings were also compared with the experimental results for the moment resistance of the connection, as shown in Table 5. The analysis of the results revealed that the ratio was in the range of 0.86 to 0.88, indicating fair agreement. These findings indicate a high level of consensus.

4 Parametric study

To investigate the effect of various parameters on the relationship, a parametric analysis based on the test specimen (Test 1) proposed by Ostrander [19] was carried out. Because the effects of the column, beam, and plate thickness were







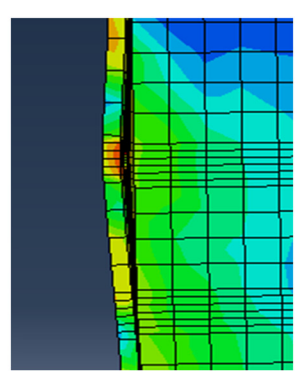


Figure 5: Deformation of connection for test specimen and FEM.



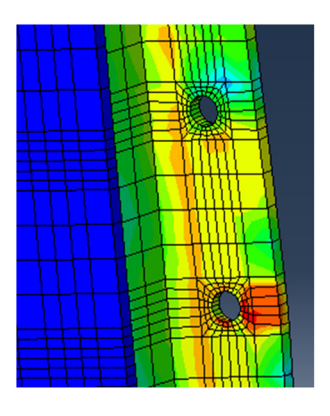


Figure 6: Yield lines for test specimen and FEM.

studied by the aforementioned author, the influence of material properties and bolt rigidity was used in this study. The parameters considered were the bolt pretension load; yield stress of the bolts; and yield stress of the column, beam, and plate.

4.1 Bolt pretension load (Tb)

The effect of adjusting the bolt pretension load on the $M-\Phi$ curve is shown in Figure 8. The moment capacity of the connection increased as the bolt pretension load increased.

Table 5: Comparison of experimental and finite element ultimate moment resistance

Test specimen	Ultimate moment, $M_{ m u}$ (kip-in)		Ratio of $M_{ m u,ABAQUS}/M_{ m u,Exp.}$	
	$M_{\mathrm{u,Exp.}}$	$M_{\rm u,ABAQUS}$		
1	538	461	0.86	
3	486	421	0.87	
4	264	233	0.88	
9	600	523	0.87	

The actions of the bolt pretension loads of 12, 20, and 30 kip are identical, with the exception of 40 kip. Figure 9(d) shows that for a bolt pretension load of 40 kip, the deformation of the connection increases, and the overall stiffness of the connection is also affected owing to the increased rigidity of the bolt in comparison with the connection materials.

4.2 Yield strength of column, beam, and plate

As shown in Figure 10, the increase in the yield stress of the column, beam, and plate materials leads to an increase in the moment capacity of the connection.

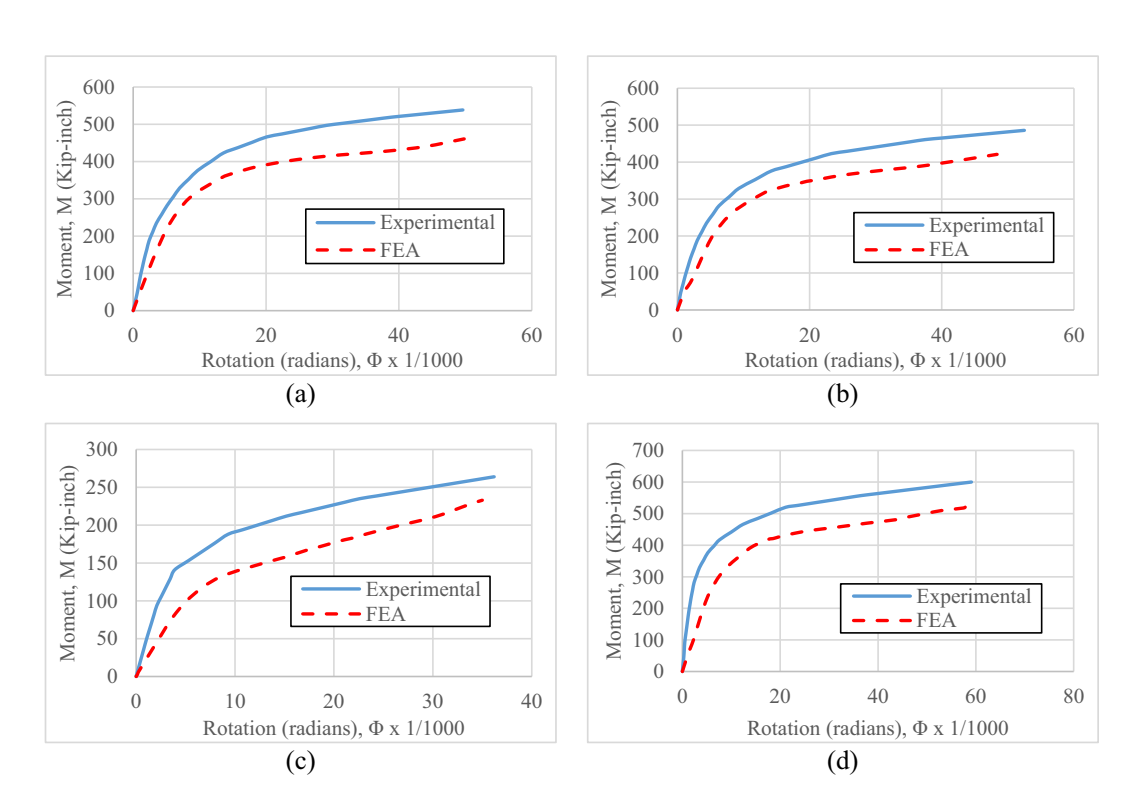


Figure 7: M- Φ curves: (a) M- Φ for Test 1, (b) M- Φ for Test 3, (c) M- Φ for Test 4, and (d) M- Φ for Test 9.

8 — Sinan A. Al-Haddad *et al.* DE GRUYTER

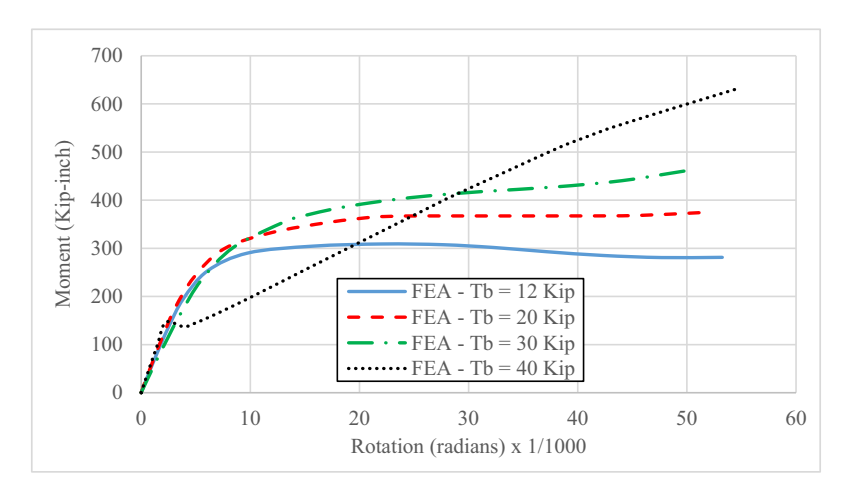


Figure 8: M-Φ curve for Test 1 with different bolt pretension loads.

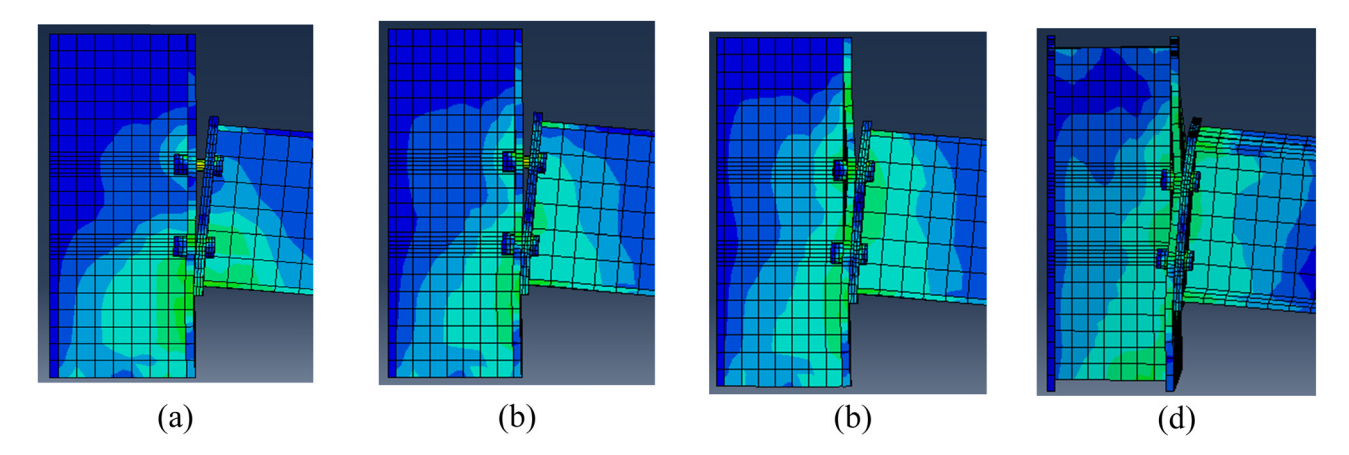


Figure 9: Deformation of connection for Test 1 with various bolt pretension loads (Tb): (a) deformation for Tb = 12 kip, (b) deformation for Tb = 20 kip, (c) deformation for Tb = 30 kip, and (d) deformation for Tb = 40 kip.

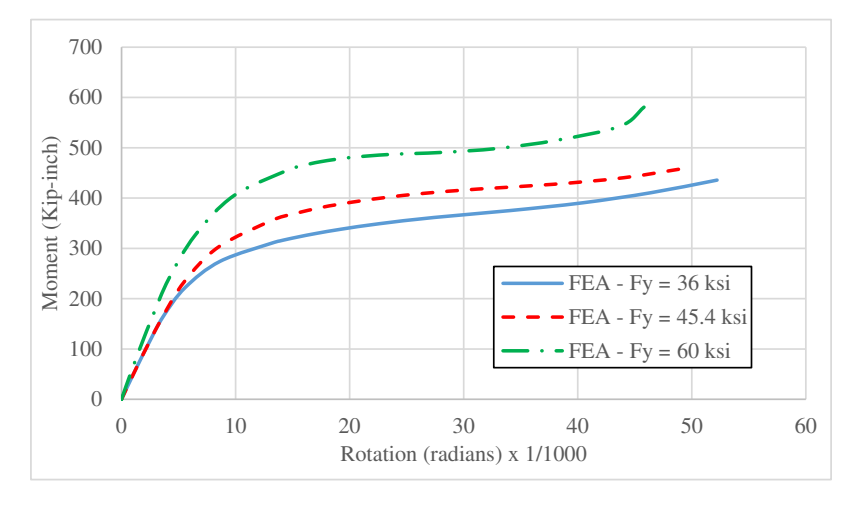


Figure 10: M-Φ curve for Test 1 with different yield stresses of column, beam, and plate.

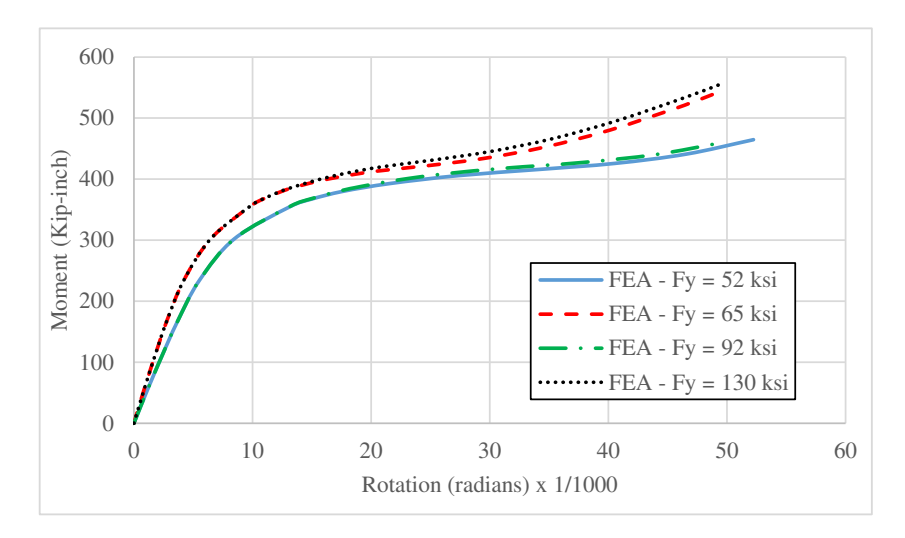


Figure 11: $M-\Phi$ curve for Test 1 with different yield stresses of bolts.

4.3 Yield stress of the bolts

The yield stress of the bolts had no considerable influence on the behavior of the connection, as shown in the $M-\Phi$ curve in Figure 11.

5 Conclusions

To analyze end-plate steel connections subjected to monotonic loads with a variety of types and features, as well as to investigate the effects of various parameters on the connection behavior, this study offers a three-dimensional FEM. The results of the study are summarized as follows:

- 1. Comparisons between the experimental and current FEM findings show that the current numerical model can mimic and forecast the behavior of bolted endplates with a fair amount of precision. The M-Φ curves were included in the comparisons.
- 2. The parametric study's findings show a strong increase in the connection's moment ability with the bolt pretension load and yield stress of the column, beam, and plate materials. The bolts' yield tension, on the other hand, has only a minor impact on the connection's moment capacity.
- 3. The study relied on a reduced number of tests, with one section for columns and beams, and a joint type. To fully evaluate the three-dimensional nature of the steel behavior of joints from beam to column, additional tests and thorough parametric analysis utilizing the nonlinear FEM are necessary for future studies.

Acknowledgement: The authors would like to thank M.H. Ehsan for his support.

Funding information: The authors state no funding involved.

Conflict of interest: The authors do not have any conflicts of interest to disclose. All co-authors have visually perceived and concurred with the substance of this manuscript, and there are no pecuniary interests to disclose.

Data availability statement: All the data, models, and codes generated or used during the study appear in the submitted article.

References

- Yorgun C, Dalcı S, Altay GA. Finite element modeling of bolted steel connections designed by double channel. Comput Struct. 2004;82(29):2563-71, https://www.sciencedirect.com/science/ article/pii/S0045794904001567.
- [2] De Santis Y, Aloisio A, Gavrić I, Šušteršič I, Fragiacomo M. Timberto-steel inclined screws connections with interlayers: Experimental investigation, analytical and finite element modelling. Eng Struct. 2023;292:116504, https://www.sciencedirect.com/science/article/ pii/S0141029623009197.
- Singh I, Stavroulakis GE, Drosopoulos GA. Impact of partially [3] damaged passive protection on the fire response of bolted steel connections using finite element analysis. Case Stud Therm Eng. 2023;49:103225, https://www.sciencedirect.com/science/article/ pii/S2214157X23005312.
- Al-Kannoon MAA, Al-Thabhawee HW. Cyclic performance of moment connections with reduced beam sections using different cut-flange profiles. 2022;12(1):691-701. doi: 10.1515/eng-2022-0354
- [5] Shi D, Huang H, Li N, Liu Y, Demartino C. Bolted steel to laminated timber and glubam connections: Axial behavior and finite-element modeling. Int J Mech Sci. 2023;252:108364, https://www. sciencedirect.com/science/article/pii/S0020740323002667.

- [6] Dabaon MA. Fundamental of steel design course and design tables. Tanta, Egypt: Tanta University; 2010.
- [7] de Construção AP. Design of steel structures: Eurocode 3: Design of steel structures, Part 1-1: General rules and rules for buildings. USA: John Wiley & Sons; 2016.
- [8] Dabaon MA, El-Boghdadi MH, El-Kasaby EA, Gerges NN. Early prediction of intimal stiffness of composite joints. In: ASCE-EGS. III Regional Conference on Civil Engineering Technology; 2002.
- [9] Mohamadi-Shoore MR, Mofid M. New modeling for moment-rotation behavior of bolted endplate connections. Sci Iran.
 2011;18(4):827–34, https://www.sciencedirect.com/science/article/ pii/S1026309811001295.
- [10] Shi Y, Shi G, Wang Y. Experimental and theoretical analysis of the moment–rotation behaviour of stiffened extended end-plate connections. J Constr Steel Res. 2007;63(9):1279–93, https://www. sciencedirect.com/science/article/pii/S0143974X06002410.
- [11] Abidelah A, Bouchaïr A, Kerdal DE. Experimental and analytical behavior of bolted end-plate connections with or without stiffeners. J Constr Steel Res. 2012;76:13–27, https://www. sciencedirect.com/science/article/pii/S0143974X1200096X.
- [12] Ismail RES, Fahmy AS, Khalifa AM, Mohamed YM. Numerical study on ultimate behaviour of bolted end-plate steel connections. Lat Am J Solids Struct. 2016;13:1–22.
- [13] Ataei A, Bradford MA, Valipour HR, Liu X. Experimental study of sustainable high strength steel flush end plate beam-to-column composite joints with deconstructable bolted shear connectors. Eng Struct. 2016;123:124–40, https://www.sciencedirect.com/ science/article/pii/S0141029616302358.
- [14] Costa R, Valdez J, Oliveira S, Simões da Silva L, Bayo E. Experimental behaviour of 3D end-plate beam-to-column bolted steel joints. Eng Struct. 2019;188:277–89, https://www.sciencedirect.com/science/article/pii/S0141029618331146.
- [15] Elflah M, Theofanous M, Dirar S, Yuan H. Behaviour of stainless steel beam-to-column joints — Part 1: Experimental investigation. J Constr Steel Res. 2019;152:183–93, https://www.sciencedirect. com/science/article/pii/S0143974X17311471.
- [16] Gao JD, Yuan HX, Du XX, Hu XB, Theofanous M. Structural behaviour of stainless steel double extended end-plate beam-to-column joints under monotonic loading. Thin-Walled Struct. 2020;151:106743. https://www.sciencedirect.com/science/article/ pii/S0263823120301956.
- [17] Saha SS, Kawshiq ASMKZ, Ahmed S. Numerical study of the behaviour of stainless steel semi-rigid joints. 6th International

- Conference on Civil Engineering for Sustainable Development, Khulna University of Engineering & Technology (KUET), Khulna, Bangladesh.
- [18] Song Y, Uy B, Li D, Wang J. Ultimate behaviour and rotation capacity of stainless steel end-plate connections. Steel Composite Struct. 2022;42(4):569–90.
- [19] Ostrander JR. An experimental investigation of end plate connections. Doctoral dissertation. University of Saskatchewan; 1970.
- [20] Chen WF. Semi-rigid connections handbook. USA: J. Ross Publishing; 2011.
- [21] Al-Haddad LA, Jaber AA. Influence of operationally consumed propellers on multirotor UAVs airworthiness: Finite element and experimental approach. IEEE Sens J. 2023;23(11):11738–45.
- [22] Fattah MY, Al-Omari RR, Ali HA. Numerical simulation of the treatment of soil swelling using grid geocell columns. Slovak J Civ Eng. 2015;23(2):9–18. doi: 10.1515/sjce-2015-0007.
- [23] Fattah MY, Salim NM, Al-Shammary WT. Effect of embedment depth on response of machine foundation on saturated sand. Arab J Sci Eng. 2015;40(11):3075–98. doi: 10.1007/s13369-015-1793-8.
- [24] Fattah MY, Majeed QG. Finite element analysis of geogrid encased stone columns. Geotech Geol Eng. 2012;30(4):713–26. doi: 10.1007/ s10706-011-9488-8
- [25] Akram H, Hilal M, Fattah M. Numerical simulation of the effect of repeated load and temperature on the behavior of asphalt layers. Eng Technol J. 2022;40(5):769–78, https://etj.uotechnology.edu.iq/ article_174578.html.
- [26] Fattah Y, MJ, Hamood M, Amoori Abbas S. Simulation of behavior of plate on elastic foundation under impact load by the finite element method. Eng Technol J. 2013;31(19):44–58, https://etj. uotechnology.edu.ig/article_83729.html.
- [27] Jaafar AA, Yussof MM, Azeez AA, Mezher TM, Ali Blash AA. The nonlinear analysis of reactive powder concrete effectiveness in shear for reinforced concrete deep beams. Open Eng. 2023;13(1):20220412. doi: 10.1515/enq-2022-0412.
- [28] Al-Haddad LA, Jaber AA, Ibraheem L, Al-Haddad SA, Ibrahim NS, Abdulwahed FM. Enhancing wind tunnel computational simulations of finite element analysis using machine learning-based algorithms. Eng Technol J. 2023;42(1):1–9. https://etj.uotechnology. edu.ig/article 181030.html.
- [29] Al-Haddad LA, Giernacki W, Shandookh AA, Jaber AA, Puchalski R. Vibration signal processing for multirotor UAVs fault diagnosis: Filtering or multiresolution analysis? Eksploatacja i Niezawodność – Maint Reliab. 2023;26(1). doi: 10.17531/ein/176318.